Journal of the Meteorological Society of Japan, Vol. 76, No. 5, pp. 675–684, 1998

Diurnal Variability of Cloudiness over East Asia and the Western Pacific Ocean as Revealed by GMS during the Warm Season

By Tomio Asai[1]

Center for Environmental Remote Sensing, Chiba University, Chiba 263-8522, Japan

Shizhao Ke

Guangdong Institute of Tropical and Marine Meteorology, Guangzhou, China

and

Yasu-Masa Kodama

Department of Earth and Environmental Sciences, Hirosaki University, Hirosaki 036-8561, Japan

(Manuscript received 15 August 1997, in revised form 8 June 1998)

Abstract

Diurnal variations of cloudiness over East Asia and the western Pacific are investigated for the warm season of 1987, based on GMS-3 IR data at every three hours. The domain chosen for the present analysis is between latitude 50°N and 20°S and longitude 90°E and 160°E.

The main results obtained are: (1) Diurnal variations of cloudiness result from superposition of large diurnal-cycle and small semidiurnal-cycle variations. Amplitude and phase of the diurnal-cycle variation are much different over land and ocean. Semidiurnal-cycle variations over land and ocean are almost in phase with maxima at 0300 ~ 0500 LT and 1500 ~ 1700 LT, and have similar amounts of amplitude. (2) A systematic phase delay of diurnal-cycle variation appears to the east of the Tibetan Plateau. A maximum of cloudiness appears near dusk over the Tibetan Plateau and at midnight in the Sichuan Basin. Phase speed of the variations is almost the same as in the eastward phase propagation of the diurnal-cycle variation of precipitation frequency east of the Rocky Mountains in the United States. Eastward movement of cloud clusters generated over the Tibetan Plateau, as well as locally induced convections, should be taken into account to understand the behavior of diurnal variation of cloudiness to the east of the Plateau. (3) The eastward phase delay of the diurnal-cycle variation to the east of the Tibetan Plateau is obscured during mid-summer. This may be caused by locally induced active convections intensified near dusk to the east of the Plateau, and seasonal disappearance of upper westerly flow passing over the Plateau.

1. Introduction

Diurnal variability of cloudiness and precipitation has been investigated in different parts of the world in different seasons. Oki and Mushiake (1994) showed a comprehensive analysis of the diurnal variability of precipitation across Japan based on ten-year AMeDAS (Automated Meteorological Data Acquisition System) data for the selected stations. Winkler *et al.* (1988) summarized the previous studies on diurnal variability of heavy precipitation in the United States. As is expected, the diurnal variation is strongest during summer and a pronounced afternoon maximum is observed in the eastern and southern parts of the United States. However, over the Great Plains of the United States active precipitation appears near midnight in summer (Wallace 1975; Eastering and Robinson 1985). Balling (1985) and Riley *et al.* (1987) pointed out summertime eastward phase propagation of the diurnal variation of precipitation between the Rocky Mountains

1 Corresponding author: Tomio Asai, Center for Environmental Remote Sensing, Chiba University, Chiba 263-8522, Japan.
Present affiliation: Japan Science and Technology Corporation, 5th Mori Bldg. 9F, 17-1, Toranomon 1-chome, Minato-ku, Tokyo 105-0001, Japan

and the Great Plains. West of the Continental Divide, a late afternoon precipitation maximum prevails. From the Continental Divide eastward to extreme western Kansas, Nebraska and South Dakota ($\sim 101°$W), the time of maximum precipitation frequency shifts consistently later to an eventual midnight (0000 LT) peak. The transition is most abrupt across eastern Colorado and extreme western portions of Nebraska and South Dakota. Eastward from 101°W, maximum frequency becomes later at a more gradual rate, reaching 0300 $\sim$ 0500 LT peak across the eastern portions of Kansas and Nebraska.

Domros and Peng (1988) summarized the climatological characteristics of the diurnal variation of precipitation over China. Precipitation is most frequently observed in the afternoon and evening in most parts of China for the major part of the year, while little precipitation occurs in the morning and at night. In May and June, however, modification of the diurnal variation of precipitation is observed in the western parts of China, particularly in Xinjiang and the Qinghai-Xizang (Tibetan) Plateau (map shown in Fig. 1). The data shows a night or early morning maximum. The diurnal variation on high mountains is characterized by a maximum precipitation during daytime, and a minimum at night. In large valleys, precipitation is less during daytime and more at night. This feature can be modified in the following two regions: in large valleys in Yunnan and Xizang, night rains follow a fine day, while in Sichuan Basin precipitation occurs at night after a cloudy day. This case is considered to be the only one in China where night precipitation significantly dominates over a large area.

Unlike the situation over land, direct measurements of precipitation over ocean are rare. Gray and Jacobson (1977) discussed a single nighttime maximum of ocean precipitation. Kraus (1963) showed that maritime precipitation in mid-latitudes was most frequent during the second half of the night, with a drop-off during the day, using nine weathership records. Recently a complex picture of the diurnal variation of oceanic rainfall activity has been shown based on satellite observations. Using three-hourly GMS-IR data and defining an intensity index of deep convective clouds, Murakami (1983) showed the maximum convective activity around 0900 $\sim$ 1200 LT over the ocean in the vicinity of large islands and around 0600 $\sim$ 0900 LT in the morning over open ocean in the tropical western Pacific. Augustine (1984) examined diurnal variation of satellite-inferred rainfall over open ocean in the tropical eastern Pacific. This exhibited dual maxima, one near dawn and the other in mid-afternoon. Using GMS-IR observations, Nitta and Sekine (1994) showed that convective activity attains its maximum in the morning over the tropical western Pacific in the vicinity of large islands,

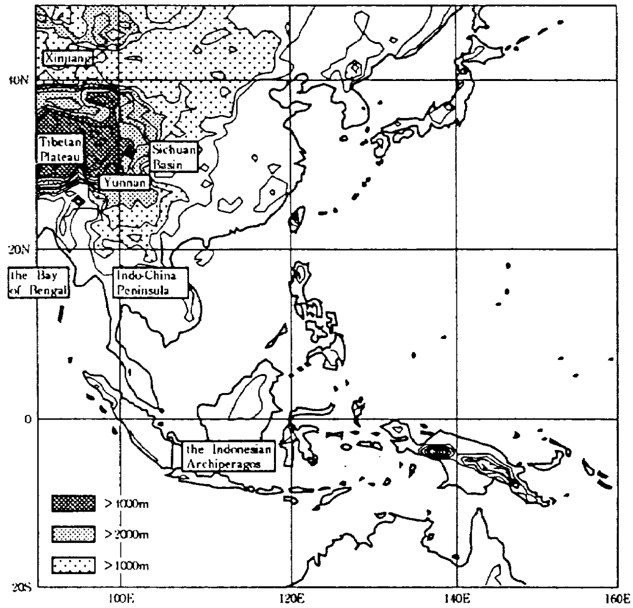

Fig. 1. Domain covering East Asia and the western Pacific Ocean adopted for the present analysis.

while it has a maximum intensity in the morning and a secondary maximum in the afternoon along the ITCZ and the SPCZ over open ocean. Chen and Takahashi (1995) showed that diurnal variation of convective activity around the South China Sea is modified by intraseasonal variations of monsoon activity.

These observational studies indicate that the diurnal variation of precipitation over ocean, especially its semidiurnal-cycle signals, is complicated and not well understood. The influence of the Tibetan Plateau on diurnal rainfall variation in China is not clarified, despite a great interest in whether eastward phase delay of diurnal variation appears to the east of the Tibetan Plateau as in the Great Plains east of the Rocky Mountains. In order to clarify these problems, we investigate diurnal variation of the amount of high-clouds, which well correlates to convective rainfall (Maruyama *et al.*, 1983) over East Asia and the western Pacific, using three hourly GMS-3 IR observations during the warm season of 1987.

2. Data and procedure for analysis

Three-hourly (0000, 0300, 0600, $\cdots$, 2100, Universal Time Coordinated) IR histogram data of GMS-3 averaged for every 0.25° longitude-latitude square mesh for the area (50°N–20°S, 90°E–160°E) shown in Fig. 1 from April to June in 1987, are used to analyze diurnal variation of cloudiness. We derived the amount of high-clouds with T_{BB} tops lower than -40°C (higher than about 400 hPa level) from the data. Hereafter, the amount of high-clouds is simply called cloudiness.

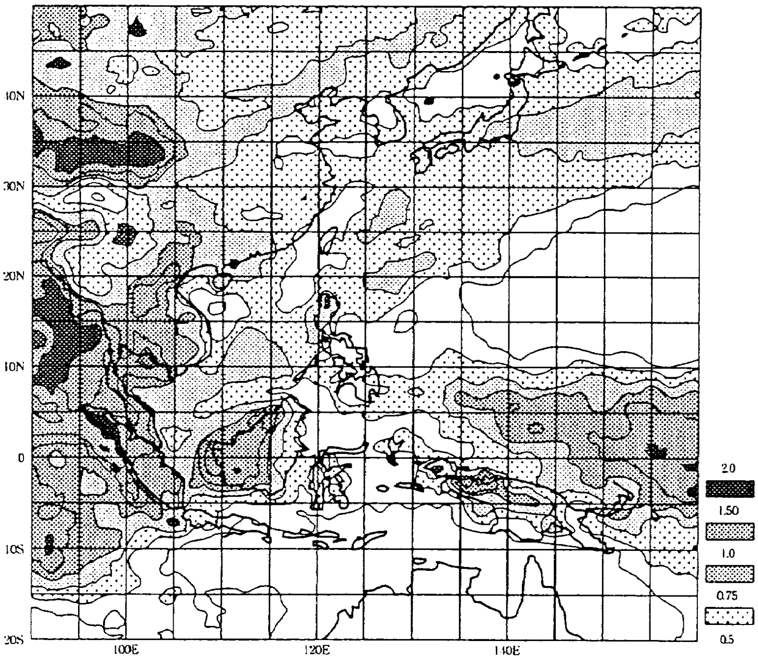

Fig. 2. Distribution of mean cloudiness of cloud tops with T_{BB} lower than $-40°C$ for the three months from April to June 1987.

Diurnal variation of cloudiness is represented by the deviation from the 24-hour mean. This is normalized by dividing it by the mean, that is,

$$Ni = (Ci - Cm)/Cm,$$

where Ci is cloudiness at a local time i and Cm is daily mean cloudiness. Fourier analysis of diurnal variation of cloudiness Ni is also made to obtain amplitude and phase of diurnal- and semidiurnal-cycle variations.

We also use a 3-hourly minimum value of T_{BB} for each 1° longitude-latitude square mesh during the warm season (April to September) of 1987 to study seasonal change of diurnal variation of cloudiness; the IR histogram data contains too much information to be analyzed for a longer period of time. Hereafter we refer to the value as min-T_{BB}, which is an indicator of cloud-top-height, because it shows the minimum cloud-top-temperature when the mesh includes some cloudy area. After eliminating the meshes with the min-T_{BB} $> -20°C$, which are shown uncovered or covered with low-level clouds, we determined the amplitude and phase of diurnal-cycle variation of the min-T_{BB} using the harmonic analysis method. NCEP (the U.S. National Centers for Environmental Prediction)/NCAR (the U.S. National Center for Atmospheric Research) re-analysis data are also utilized to describe atmospheric circulation.

3. Diurnal variation of cloudiness over land and ocean

Distribution of mean cloudiness between April and June, 1987 is shown in Fig. 2. Large-cloudiness zones are found around the equator and the mid-latitudes, which correspond to the ITCZ and the Baiu frontal zone respectively, while small-cloudiness areas are found in the subtropical high-pressure belts located in the subtropics. Other remarkable large-cloudiness areas are observed in the Tibetan Plateau, the Indo-China Peninsula, the Bay of Bengal and the Indonesian Archiperagos. These features are the same as known climatologically.

Figure 3 shows distribution of the normalized diurnal variation of cloudiness (Ni) averaged in every 5° longitude-latitude square mesh in the whole domain. Diurnal variation is larger over land, particularly over the Tibetan Plateau and the Indo-China Peninsula, than over ocean. Low ground-surface temperature of the Tibetan Plateau does not contaminate our evaluation of cloudiness, because only high-clouds with top temperature lower than $-40°C$ are analyzed. Over land amplitudes of diurnal variation are large in areas with large cloudiness, while small amplitudes are found in the areas with large cloudiness over ocean, such as in the ITCZ, Baiu frontal zone and the Bay of Bengal. These features are consistent with the previous studies (Murakami 1983; Nitta and Sekine 1994; Chen and Takahashi 1995).

Diurnal variations of mean cloudiness over land (thick line) and over ocean (thin line) for each month are shown in Fig. 4. Here the cloudiness over land (ocean) is averaged for all of the 1° longitude-latitude square meshes in which land (ocean) covers more than half of the area. Table 1 repre-

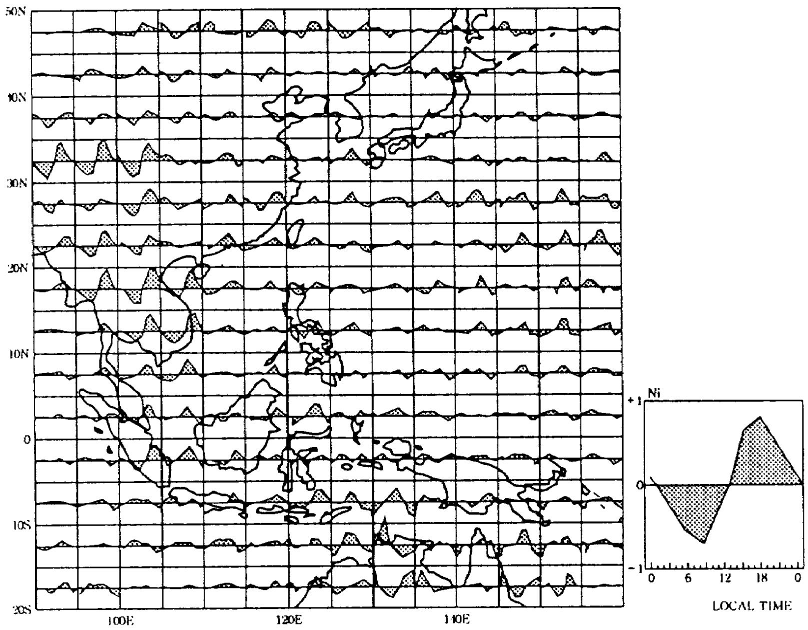

Fig. 3. Normalized diurnal variations of cloudiness in each 5° longitude- latitude square averaged for the three months from April to June 1987.

sents amplitudes and phases of diurnal-cycle and semidiurnal-cycle variations of the cloudiness over land and ocean derived by Fourier analysis for each month, though characteristics of the diurnal variations change locally within land or ocean. Unique diurnal variations of cloudiness are shown around tropical coasts (*e.g.*, Murakami 1983; Nitta and Sekine 1994) and to the east of the Tibetan Plateau in China (shown in the next section). Nevertheless, Fig. 4 and Table 1 are useful to describe the characteristics of the diurnal variations generally observed over land and ocean.

Over land (ocean), the maximum cloudiness appears around 1800 LT (1500 LT) and the minimum around 1000 LT (2100$\sim$0000 LT) every month. Table 1 suggests that the maximum and the minimum cloudiness result from superposition of large diurnal- and small semidiurnal-cycle variations. The amplitude of diurnal-cycle variation is about two times larger over land than over ocean. The phase of the diurnal-cycle variation over land is also different from those exhibited over ocean. On the other hand, differences in the amplitude and the phase of semidiurnal-cycle variation are small between over land and ocean. The amplitude and the phase are somewhat larger and later, respectively, over land. Since the amplitude of the diurnal-cycle variation is not so large over ocean, a secondary peak of cloudiness appears in the morning ($\sim$0600 LT) accompanied with the semidiurnal-cycle variation over ocean (Fig. 4).

Nitta and Sekine (1994) pointed out that there exist semidiurnal-cycle variations of convection

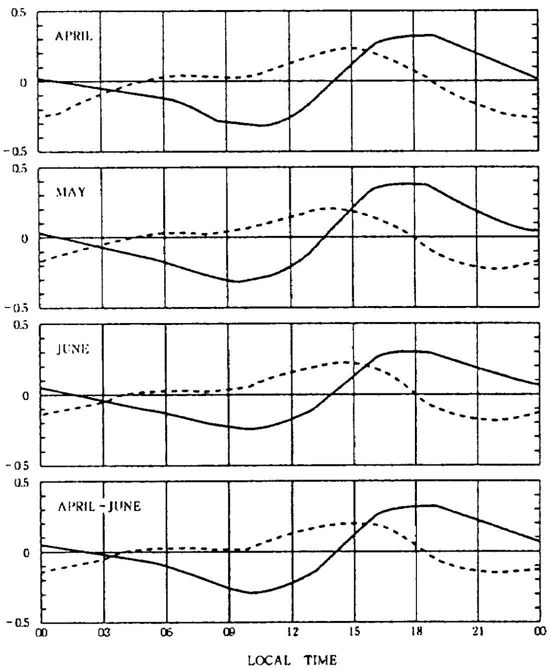

Fig. 4. Normalized diurnal variations of cloudiness over land (solid line) and ocean (broken line) for each month between April and June 1987 except for the bottom panel, averaged for the three months.

with maximum peaks around 0300$\sim$0400 LT and 1500$\sim$1600 LT along the ITCZ and the SPCZ over the western Pacific. Augustine (1984) also showed semidiurnal-cycle variations in satellite-

Table 1. The amplitudes and phases of diurnal-cycle and semidiurnal-cycle variations of cloudiness derived by Fourier analysis.

	period	one day		a half day	
		amp.	phase	amp.	phase
land	April–June	0.25	20:08	0.11	5:20/17:20
	April	0.27	20:08	0.12	5:44/17:44
	May	0.29	19:36	0.12	5:10/17:10
	June	0.23	19:48	0.09	5:10/17:10
sea	April–June	0.14	12:20	0.08	3:36/15:36
	April	0.18	13:08	0.09	4:48/16:48
	May	0.16	11:44	0.08	3:26/15:26
	June	0.15	12:20	0.07	3:20/15:20

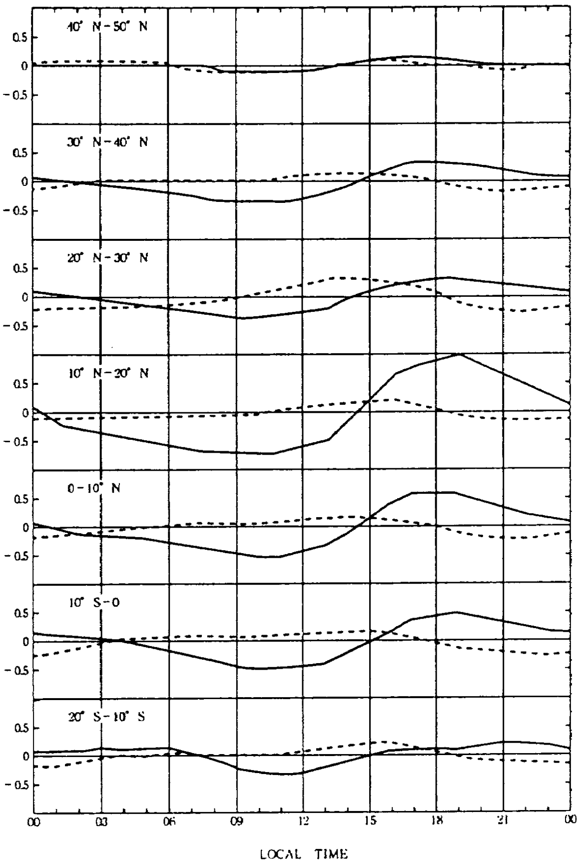

Fig. 5. Normalized diurnal variations of cloudiness at every 10° latitudinal belt over land (solid line) and ocean (broken line) averaged for the three months from April to June 1987.

inferred rainfall over the eastern Pacific with maximum peaks around 0400 ~ 0500 LT and 1600 ~ 1700 LT. Asai and Nakai (1979) found semidiurnal-cycle variations of cloudiness observed on the R. V. "Hakuho-maru," with maximum peaks at ~ 0500 LT and 1700 ~ 1800 LT over the tropical western Pacific. Our result well agrees with these studies in spite of different definitions and observation methods of cloudiness or convective activities in Nitta and Sekine (1994), Augustine (1984), Asai and Nakai (1979), and our study.

Figure 5 shows latitudinal change of mean cloudiness variations over land (solid line) and ocean (broken line) for the period from April to June 1987. Over land, the maximum of cloudiness at ~ 1800 LT is observed in every latitude, though amplitude is larger at lower latitudes. Over ocean, the primary maximum at ~ 1500 LT is observed at every latitude, while the secondary maximum in the morning is significant only around the equator (10°N ~ 10°S).

Brier and Simpson (1969) found semidiurnal-cycle variations with maxima around 0800 LT and 2000 LT in the long-term records of rainfall frequency and cloudiness at the two observation stations in the tropics. They related this variation to the semidiurnal-cycle variation of tidal convergence in the atmosphere with maximum peaks around 0800 LT and 2000 LT. There is a three-hour phase difference in the semidiurnal-cycle variations between Brier and Simpson (1969) and our study. The peaks of semidiurnal-cycle cloudiness variations in our study appear when sea level pressure is minimum in the atmospheric tide around 0400 LT and 1600 LT. Our results, therefore, may hardly be related to atmospheric tidal convergence.

Gray and Jacobson (1977) showed that deep cumulus convection is intensified in the morning in many places over both land and ocean. They proposed a possible explanation. Since nighttime radiative cooling is weaker in convective cloud systems than in surrounding cloud-free regions, a convergent flow toward the convective cloud systems is intensified by temperature differences between the systems and their surrounding regions. Their explanation, however, is difficult to apply to the afternoon maximum of observed ocean cloudiness. Further studies are necessary to clarify the mechanisms of the semidiurnal variation of cloudiness.

4. Diurnal variation of cloudiness over China

The amplitude and phase of the normalized diurnal-cycle variations in cloudiness for the three months from April to June 1987 are represented using wind notation in Fig. 6. Phase is indicated by wind direction, *e.g.*, the north wind indicates a midnight (0000 LT) maximum, the west wind indicates a 1800 LT maximum, *etc.* Amplitude is indicated by the wind speed. Over the Tibetan Plateau peaks of cloudiness appear near dusk (~ 1800 LT) and delay as they move eastward. According to surface cloud-type observations in the Tibetan Plateau, Cb clouds frequently appear throughout the year especially after April during the warm season (Institute of Meteorological Science of Qinghai Province 1986).

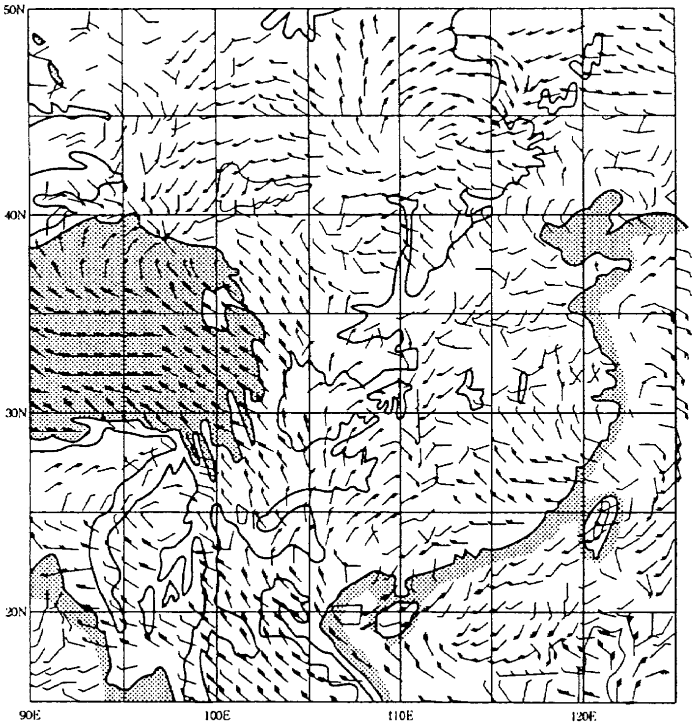

Fig. 6. Amplitude and phase of the diurnal-cycle variation of cloudiness over China derived by Fourier analysis for the three months from April to June 1987. Each full barb and pennant represent 0.2 and 1.0 in amplitude of diurnal-cycle variation of cloudiness, respectively. An arrow pointing from the north indicates a midnight maximum (0000 LT) and one pointing from the east indicates a 0600 LT maximum, *etc.* Contours are drawn at 1000 m and 3000 m above sea-level topography. Shading indicates the areas with high altitudes of ground-surface exceeding 3000 m, and the positions of coast lines.

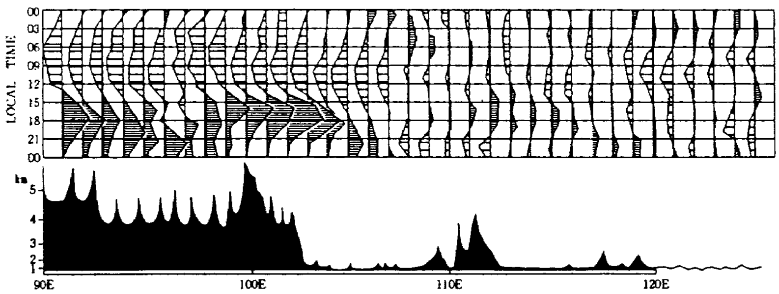

Fig. 7. Diurnal variation of cloudiness (upper panel) and topography (lower panel) along 30°N in China. 1 degree in longitude corresponds to a scale of 0.5 anomaly of cloudiness. Positive (negative) anomaly of cloudiness is thick (thin) hatched.

Diurnal variations of Cb clouds may cause the diurnal variation of satellite-observed cloudiness over the Plateau, although we cannot specify the dominant cloud types over the Plateau by GMS observations.

Figure 7 shows topography and cloudiness variation along 30°N in China. To the east of the edge of the Tibetan Plateau at 105°E, eastward phase delay is significant. Around mountainous area at $\sim 110°$E, two peaks appear in the diurnal variation of cloudiness; one is early in the morning and the other late in the afternoon to early evening. The former is likely advected from the Plateau and the latter may be locally generated just after sunset. Both the cloud cluster produced by the eastward advection of convective systems, and locally generated convective systems, should be taken into account in the diurnal cycle of cloudiness to the east of the Tibetan Plateau.

Distributions of the phases and the amplitudes indicated by wind notation of diurnal variations of the min-T_{BB} in China, and of precipitation frequency in the United States after Riley *et al.* (1987),

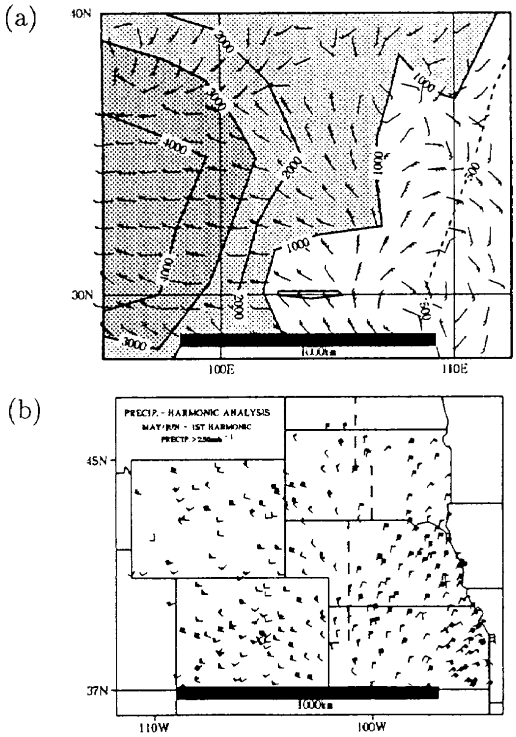

Fig. 8. (a) Same as in Fig. 6 except for the min-T_{BB} in $1° \times 1°$ grid over China for the two months from April to May, 1987. Each barb and pennant represent 2 K and 10 K in amplitude of diurnal variation, respectively. An arrow pointing from the north indicates a midnight minimum (0000 LT) and one pointing from the east indicates a 0600 LT minimum, *etc.* (b) Diurnal variation in the frequency of all measurable precipitation (> 0.25 mm) in North America for early summer (May–June). (From Riley *et al.*, 1987).

are shown in Fig. 8 to compare diurnal variations of cloudiness in China and of precipitation in the United States. Phase of the min-T_{BB} indicates the time when the min-T_{BB} is minimum, *i.e.*, cloud-top-height is maximum in the diurnal-cycle variation. Over the Tibetan Plateau, where land-surface temperature sometimes falls below the threshold value of the min-T_{BB} ($-20°$C), the low surface temperature may contaminate the min-T_{BB}. However, the minimum of the min-T_{BB} is observed not at dawn, when the minimum land-surface temperature is observed, but near dusk when the peaks of cloudiness appear (Fig. 6). Therefore, diurnal variation of the min-T_{BB} over the Plateau represents not the variations of the land-surface temperature, but of cloudiness.

The eastward progresses of the phase from the Tibetan Plateau and from the Rocky Mountains are significant. Phase speed to the east of the Plateau is almost as much as over the Great Plains. Over the Tibetan Plateau, the minimum is observed at dusk in the same fashion as the Rocky Mountains where the maximum precipitation frequency appears near dusk. Over Sichuan Basin ($\sim 30°$N and $\sim 105°$E), the minimum phase of the min-T_{BB} is observed at midnight.

Figure 9 shows diurnal variations of the min-T_{BB} along 30°N in each month during the warm season of 1987. Eastward phase propagation of negative anomaly of the min-T_{BB} from the Tibetan Plateau is significant except during the mid-summer of July and August. Riley *et al.* (1987) showed that the eastward phase propagation of rainfall from the Rocky Mountains is observed between May and August, including mid-summer. Before April and after September, the maximum rainfall appears from midnight to early morning in most parts of the Rocky Mountains and the Great Plains. Evening maximum (~ 1800 LT) over the Rocky Mountains appears only between May and August. Over the Tibetan Plateau, on the other hand, active development of deep convective clouds in the evening is observed throughout the warm season. Nevertheless, the eastward phase propagation to the east of the Plateau is obscure in mid-summer.

Figure 9 represents that diurnal variation in China to the east of the Tibetan Plateau result from superposition of eastward advection of convective clouds generated over the Plateau and of locally induced convections near dusk (~ 1800 LT). The latter is significant during mid-summer and covers the eastward propagation of cloudiness. Figures 10a and 10b show 500 hPa wind fields over China for April and May, and for July and August, respectively, in 1987 derived from the NCEP/NCAR re-analysis data. In the former period, strong westerly wind of ~ 10 m/s prevails both over and to the east of the Plateau. The wind-speed in the mid-troposphere almost agrees with the phase speed of the eastward propagation of cloudiness to the east of the Plateau. As is known climatologically, the westerly wind over the Plateau disappears in mid-summer. This circumstance may result in the disappearance of the eastward phase propagation by ceasing the eastward advection of convective clouds generated over the Plateau.

Figures 10c and 10d show the long-term averaged wind fields at 500 hPa over North America for April and May, and for July and August, respectively. Over North America, the westerly wind becomes as weak over a broad area to the south of 35°N in mid-summer as over China. However, the westerly wind passing over the Rocky Mountains remains even in mid-summer in the mid-latitudes to the north of 35°N, because the Rocky Mountains extend to higher latitudes than the Tibetan Plateau. The westerly wind may sustain the eastward advection of convective clouds from the Rocky Mountains

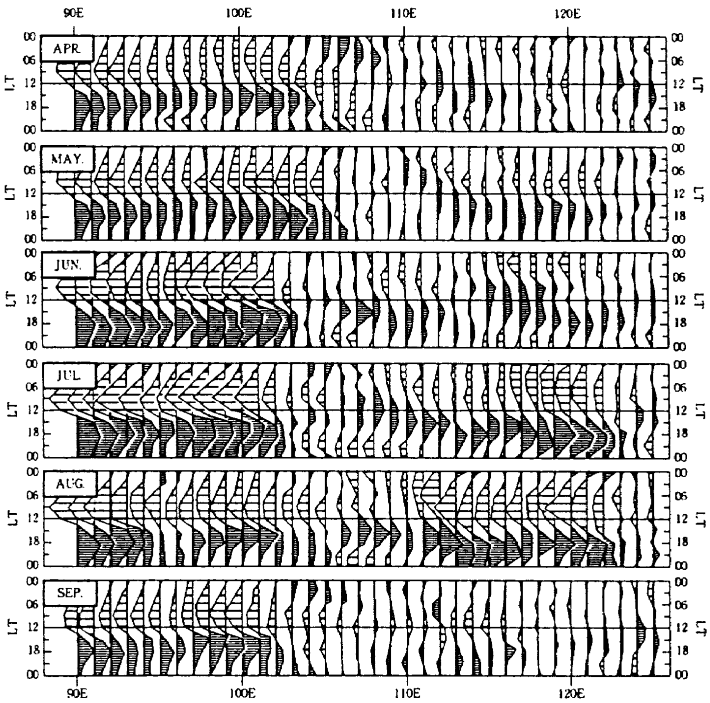

Fig. 9. Diurnal variation of the min-T_{BB} along 30°N in China averaged for each month between April and September 1987. Negative (positive) anomalies of the min-T_{BB} from the daily mean are thick (thin) hatched. 1 degree in longitude corresponds to a scale of 8°C in the anomaly of the min-T_{BB}.

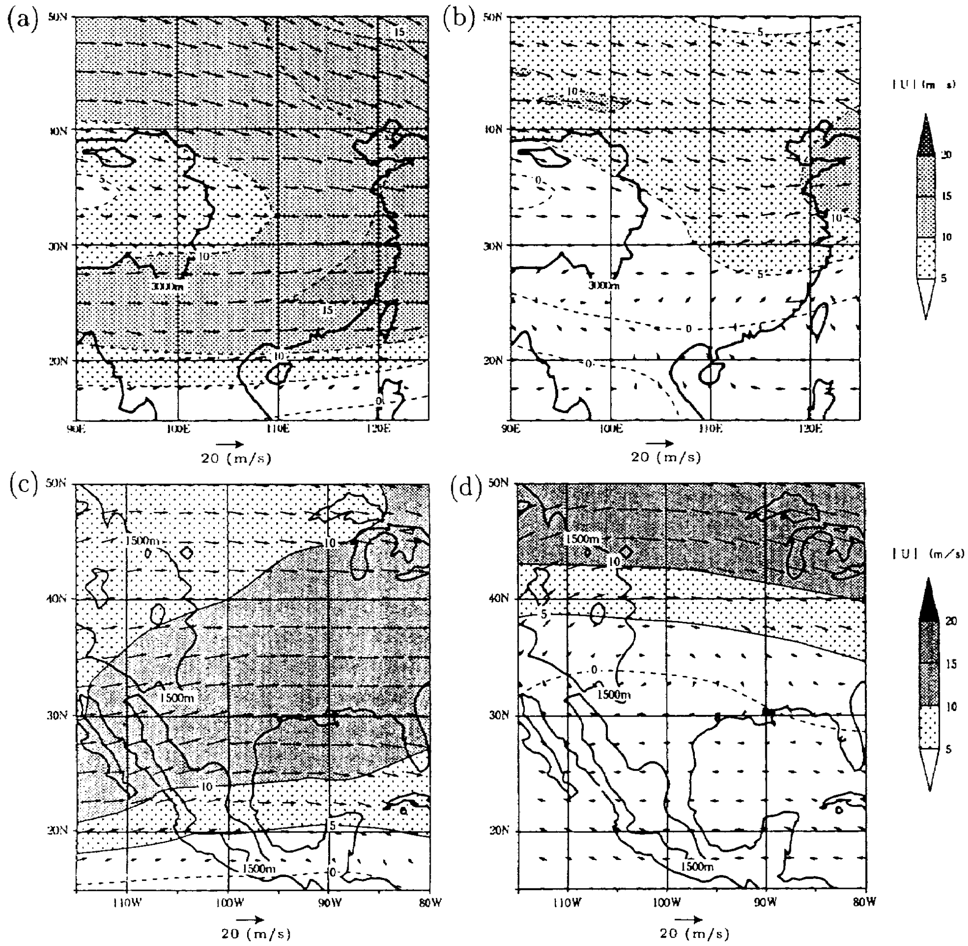

Fig. 10. (a) Wind fields at 500 hPa level over China averaged for April and May, 1987. Contour with shading indicates the eastward component (u) of wind. (b) The same as (a) except for July and August, 1987. (c) The same as (a) except over North America averaged for April and May for the eight years from 1986 to 1993. (d) The same as (c) except for July and August.

over the latitude range shown in Fig. 8b.

5. Summary and conclusion

Diurnal-cycles of cloudiness over East Asia and the western Pacific Ocean are investigated for the warm season from April to September in 1987, based on GMS-3 IR data at every three hours.

The main results obtained are as follows:

(1) Diurnal variations of cloudiness have 1.5 times larger amplitudes over land than over ocean. The maximum of cloudiness is observed at 1500 LT over ocean and 1800 LT over land. Around the equator (10°N $\sim$ 10°S), the secondary maximum appears in the morning over ocean. Amplitudes of diurnal variations of cloudiness are bigger in larger mean cloudiness over land, while they are smaller in larger mean cloudiness over ocean.

(2) Diurnal variations of cloudiness result from superposition of large diurnal-cycle and small semidiurnal-cycle variations. Amplitude and phase of the diurnal-cycle variation are much different between over land and ocean. The semidiurnal-cycle variations over land and ocean are almost in phase with maximums at 0300 $\sim$ 0500 LT and 1500 $\sim$ 1700 LT and have similar amounts of amplitude, though the amplitude and the phase are somewhat larger and later over land.

(3) A systematic phase delay of diurnal-cycle variation appears to the east of the Tibetan Plateau. A maximum cloudiness appears near dusk ($\sim$ 1800 LT) over the Tibetan Plateau and at midnight in the Sichuan Basin. Phase speed of the variations is almost as much as that in the eastward propagation observed to the east of the Rocky Mountains. Eastward movement of cloud clusters generated over the Tibetan Plateau as well as topographical effects should be taken into account to understand the behavior of diurnal variation of cloudiness to the east of the Plateau.

(4) The eastward phase delay of the diurnal-cycle variation to the east of the Tibetan Plateau is obscure during mid-summer. Locally induced active convections intensified near dusk to the east of the Plateau, and seasonal disappearance of upper westerly wind passing over the Plateau contribute to the disappeared phase propagation.

Acknowledgments

The authors thank Dr. M. Murakami and Mr. K. Takahashi, Meteorological Research Institute, JMA for providing GMS T_{BB} data. We utilized the reanalysis data of NCEP/NCAR obtained from the data library of NCAR and compiled by Mr. A. Shinpo and Dr. H. Nakamura, Graduate School of Science, the University of Tokyo. The authors wish to extend their thanks to Dr. S. Tao, Institute of Atmospheric Physics, Academia Sinica, Beijing for making helpful comments on their manuscript.

References

Asai, T. and T. Nakai, 1979: A brief summary of the weather situation during the MONEX Cruise. Preliminary Report of the Hakuho Maru Cruise KH-79-2 (MONEX Cruise) (T. Asai, ed.), Ocean Research Institute, the University of Tokyo, 5-10.

Augustine, J.A., 1984: The diurnal variation of large-scale inferred rainfall over the tropical Pacific Ocean during August 1979. *Mon. Wea. Rev.*, **112**, 1745–1751.

Balling, R.C., 1985: Warm season nocturnal precipitation in the Great Plains of the United States. *J. Climate and Appl. Meteor.*, **24**, 1383–1387.

Brier, G.W. and J. Simpson, 1969: Tropical cloudiness and rainfall related to pressure and tidal variations. *Quart. J. Roy. Meteor. Soc.*, **95**, 120–147.

Chen, T.-C. and K. Takahashi, 1995: Diurnal variation of outgoing longwave radiation in the vicinity of the South China Sea: Effect of intraseasonal variation. *Mon. Wea. Rev.*, **123**, 566–577.

Domros, M. and G. Peng, 1988: *The climate of China.* Springer-Verlag, 360pp.

Easterling, D.R. and P.J. Robinson, 1985: The diurnal variation of thunderstorm activity in the United States. *J. Climate and Appl. Meteor.*, **24**, 1048–1058.

Gray, W.M. and R.W. Jacobson, 1977: Diurnal variation of deep cumulus convection. *Mon. Wea. Rev.*, **105**, 1171–1188.

Institute of Meteorological Science of Qinghai Province, 1986: *Atlas of clouds over the Qinghai-Xizang plateau.* Science Press, Beijing, China, 212pp.

Kraus, E.B., 1963: The diurnal precipitation change over the sea. *J. Atmos. Sci.*, **20**, 551–556.

Maruyama, T., T. Nitta and Y. Tsuneoka, 1986: Estimation of monthly rainfall from satellite-observed cloud amount in the tropical Pacific. *J. Meteor. Soc. Japan*, **64**, 147–153.

Murakami, M., 1983: Analysis of deep convective activity over the western Pacific and Southeast Asia, Part I: Diurnal variation. *J. Meteor. Soc. Japan*, **61**, 60–76.

Nitta, T. and S. Sekine, 1994: Diurnal variation of convective activity over the tropical western Pacific. *J. Meteor. Soc. Japan*, **72**, 627–641.

Oki, T. and K. Mushiake, 1994: Seasonal change of the diurnal cycle of over Japan and Malaysia. *J. Appl. Meteor.*, **33**, 1445–1463.

Riley, G.T., M.G. Landin and L.F. Bosart, 1987: The diurnal variability of precipitation across the central Rockies and adjacent Great Plains, 1987. *Mon. Wea. Rev.*, **115**, 1161–1172.

Wallace, J.M., 1975: Diurnal variations in precipitation and thunderstorm frequency over the conterminous United States. *Mon. Wea. Rev.*, **103**, 406–419.
Winkler, J.A., B.R. Skeeter and P.D. Yamamoto,1988: Seasonal variations in the diurnal characteristics of heavy hourly precipitation across the United States. *Mon. Wea. Rev.*, **116**, 1641–1658.

静止気象衛星観測に基づく東アジア・西太平洋における暖候期の雲量の日変化

浅井冨雄[1]
（千葉大学環境リモートセンシング研究センター）
柯　史釗
（廣東熱帯海洋気象研究所）
児玉安正
（弘前大学理工学部）

1987年の暖候期について東アジア・西太平洋上の雲の日変化を静止気象衛星「ひまわり」3号の赤外放射観測資料を用いて調べた。調査対象領域は北緯50度から南緯20度、東経90度から160度の範囲である。得られた主な結果は以下の通りである。

(1) 雲量日変化は大きな1日周期変動と小さな半日周期変動から成る。1日周期変動の振幅と位相は陸上と海上で大きく異なるが、半日周期変動の振幅と位相は陸上と海上で類似している。半日周期変動の雲量の極大は、地方時の3時～5時と15時～17時にみられる。(2) 日周変化の位相の系統的なずれがチベット高原からその東方の中国大陸上でみられる。すなわち、雲量の極大はチベット高原上では夕方に、四川盆地では真夜中に現れる。日周変化の位相の東進速度は北米ロッキー山脈の東方でみられる降水頻度の日周変化のそれに類似している。局地的に誘起される対流活動に加えて、チベット高原で形成する雲クラスターの東進は中国大陸上の雲の日変化を理解するためには考慮されるべきであろう。(3) チベット高原の東方の中国大陸で日周変化の位相の東進は盛夏期に不明瞭になる。これは主に中国大陸で夕方局地的に発達する対流とチベット高原越えの上層偏西風の衰弱によると推測される。

[1]現在所属：科学技術振興事業団